

SUPPLEMENTAL INFORMATION

Use of Oppositely-Polarized External Magnets to Improve the Accumulation and Penetration of Magnetic Nanocarriers into Solid Tumors

Jessica F. Liu[†], Ziyang Lan[†], Carolina Ferrari[†], Joel M. Stein[‡], Elizabeth Higbee-Dempsey^{†§}, Lesan Yan[†], Ahmad Amirshaghghi[†], Zhiliang Cheng[†], David Issadore^{†,}, Andrew Tsourkas^{†,*}*

[†]Department of Bioengineering, School of Engineering and Applied Sciences, University of Pennsylvania, Philadelphia, Pennsylvania 19104, United States

[‡]Department of Radiology, Division of Neuroradiology, Hospital of the University of Pennsylvania, Philadelphia, Pennsylvania 19104, United States

[§]Biochemistry and Molecular Biophysics Graduate Group, Perelman School of Medicine, University of Pennsylvania, Philadelphia, Pennsylvania 19104, United States

210 S. 33rd St. Philadelphia, PA 19104, United States

atsourk@seas.upenn.edu, issadore@seas.upenn.edu

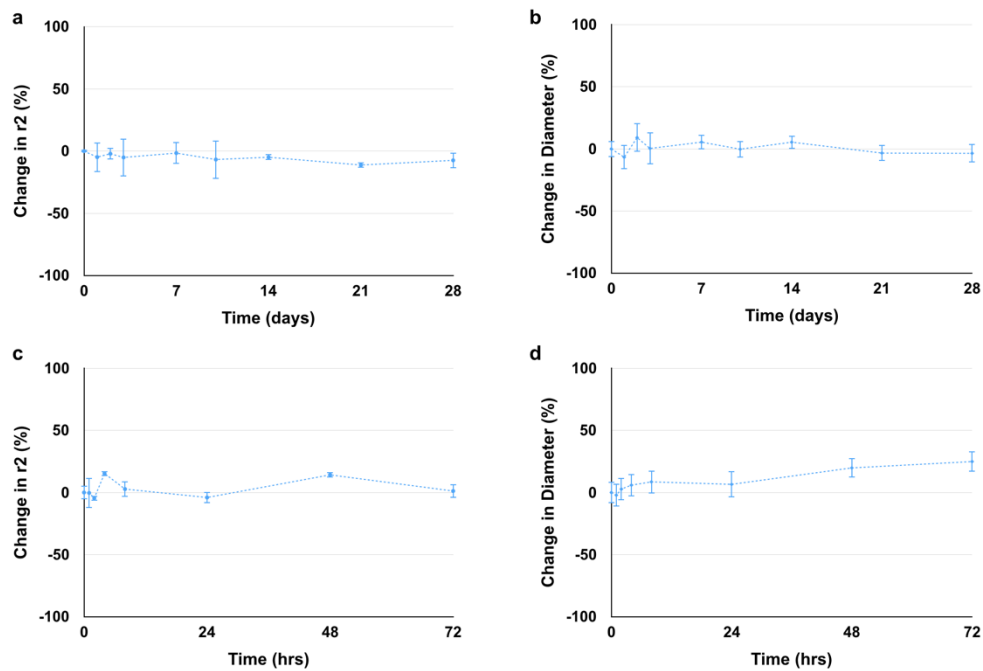


Figure S1. The SPION micelles are stable in FBS at 37°C for 72 hours, and in PBS at 4°C for up to 1 month. (a) The r2 of the micelles is stable in PBS at 4°C for 28 days. (b) The diameter of the micelles is stable in PBS at 4°C for 28 days. (c) The r2 of the micelles is stable in FBS at 37°C. (d) The diameter of the micelles increases slightly over time in FBS at 37°C, likely due to the accumulation of a protein shell around the particles.

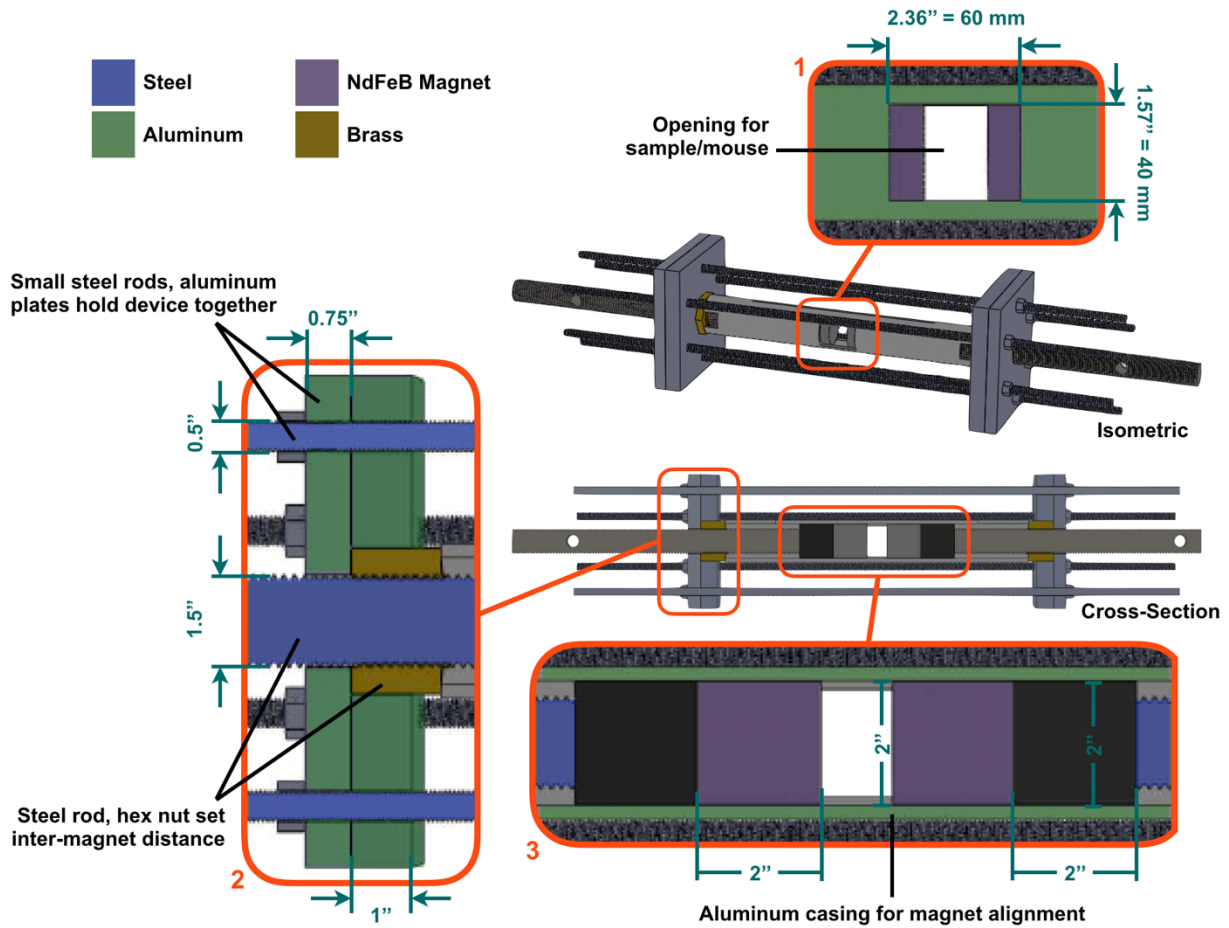


Figure S2. The magnetic device comprises two oppositely polarized static magnets aligned within an aluminum tube. The aluminum tube has an open window into which samples and animals can be placed (1). The intermagnet distance is controlled using 1.5'' diameter steel threaded rods in brass hex nuts (2). These materials were chosen to minimize the risk of friction welding. The brass hex nuts are held in place against aluminum end plates held together at a fixed distance by smaller steel rods (2). The active magnetic region of the device is constructed using 2'' diameter \times 2'' height NdFeB rare earth element magnets (3). The magnets are cushioned by a rubber stopper on each end to distribute the force applied by the threaded steel rods, to prevent physical damage from the threaded steel rods, and to minimize magnetic interactions between the magnets and the steel.

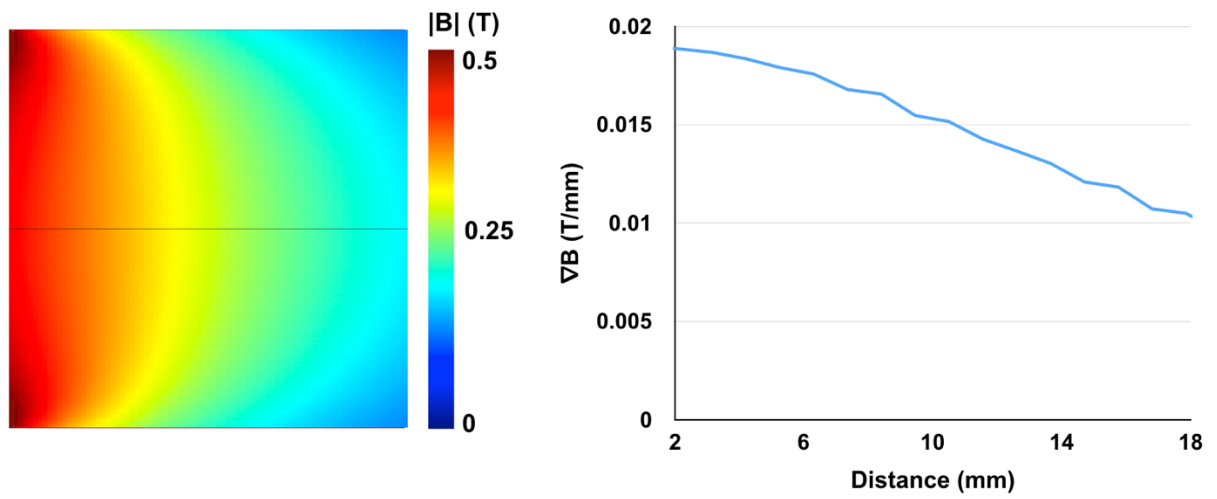


Figure S3. The magnetic field gradient drops off rapidly in single magnet systems. (a) COMSOL simulation of magnetic field in single magnet system. (b) Unlike in two magnet systems, where the gradient is constant, in this system the field drops off rapidly with distance from the magnet.

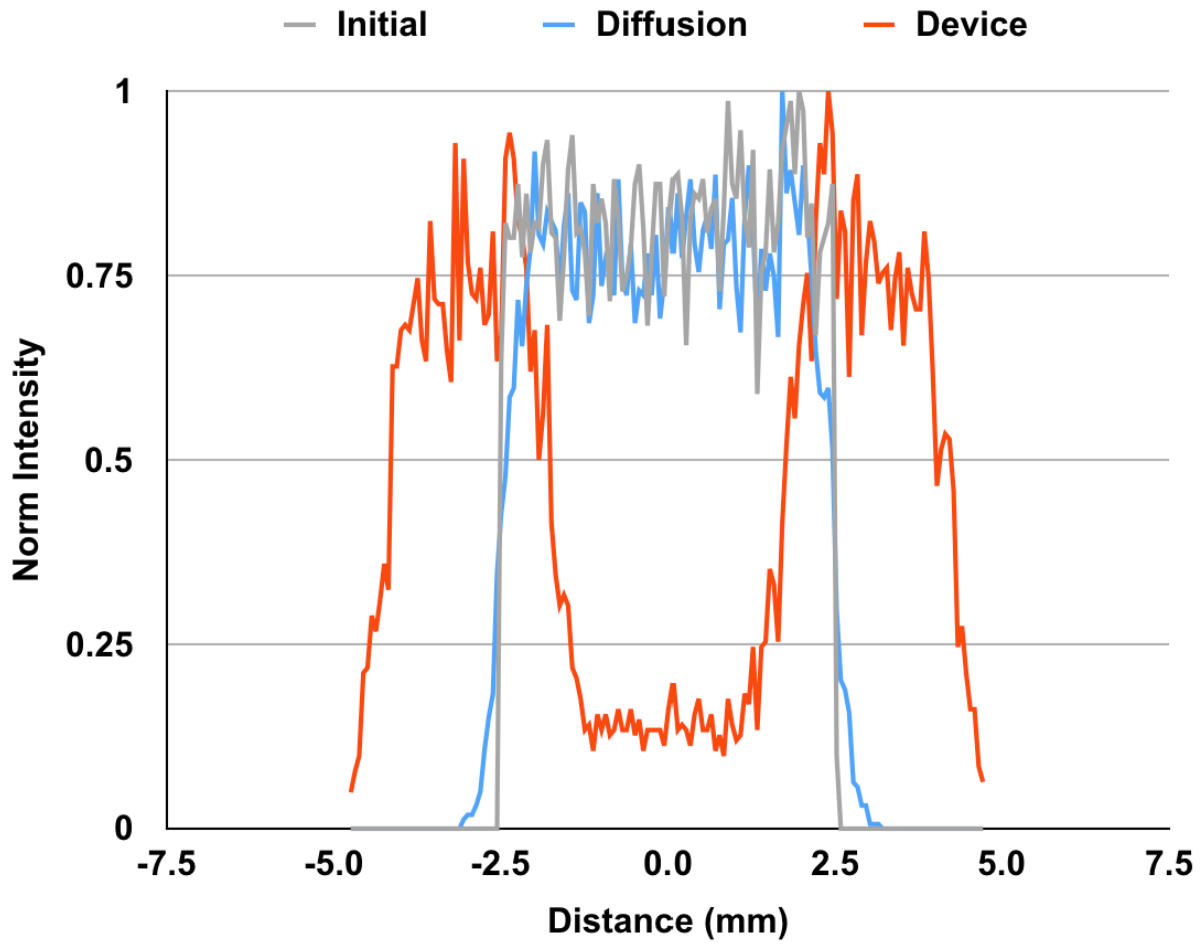


Figure S4. Simulations of particle movement through a viscous gel by diffusion alone and as a result of the device exposure for 24 hours. While the diffusion profile is similar to the initial profile, the device has radially dispersed the particles. This is consistent with experimental data.

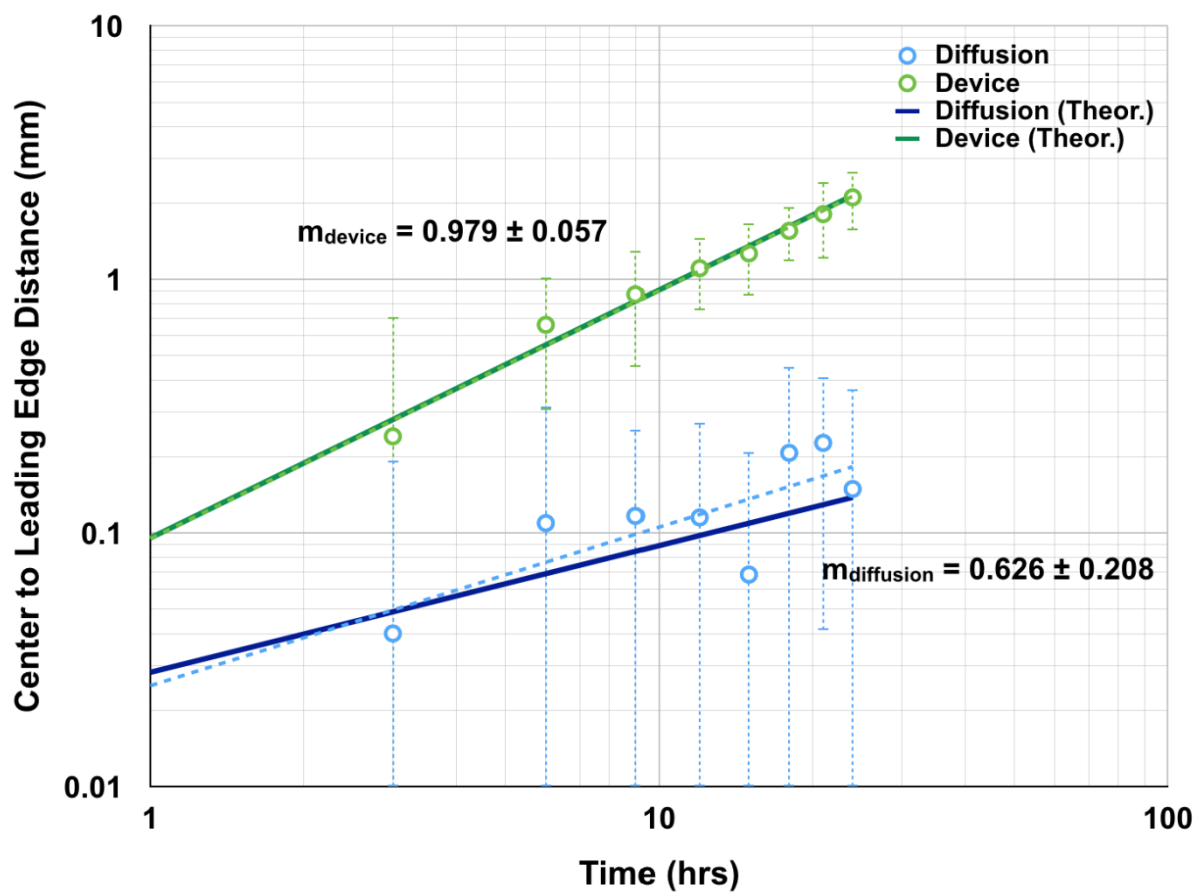


Figure S5. SPION micelle movement through the gel is well-described and linear with time. Diffusion through the gel by SPION micelles is approximately proportional to $t^{1/2}$. However, movement within the device is proportional to t . This is consistent with theoretical predictions of mass transport within a viscous medium. $N = 4$.

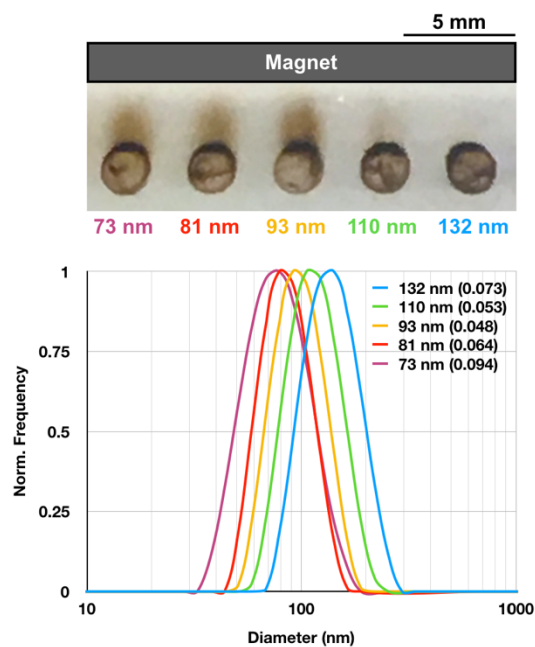


Figure S6. SPION micelle penetration through a 0.4% agarose gel phantom is dependent on micelle size. At 110 nm, there is some movement of micelles through the gel; above 110 nm, no movement is seen. DLS data are presented as average size by intensity (PDI).

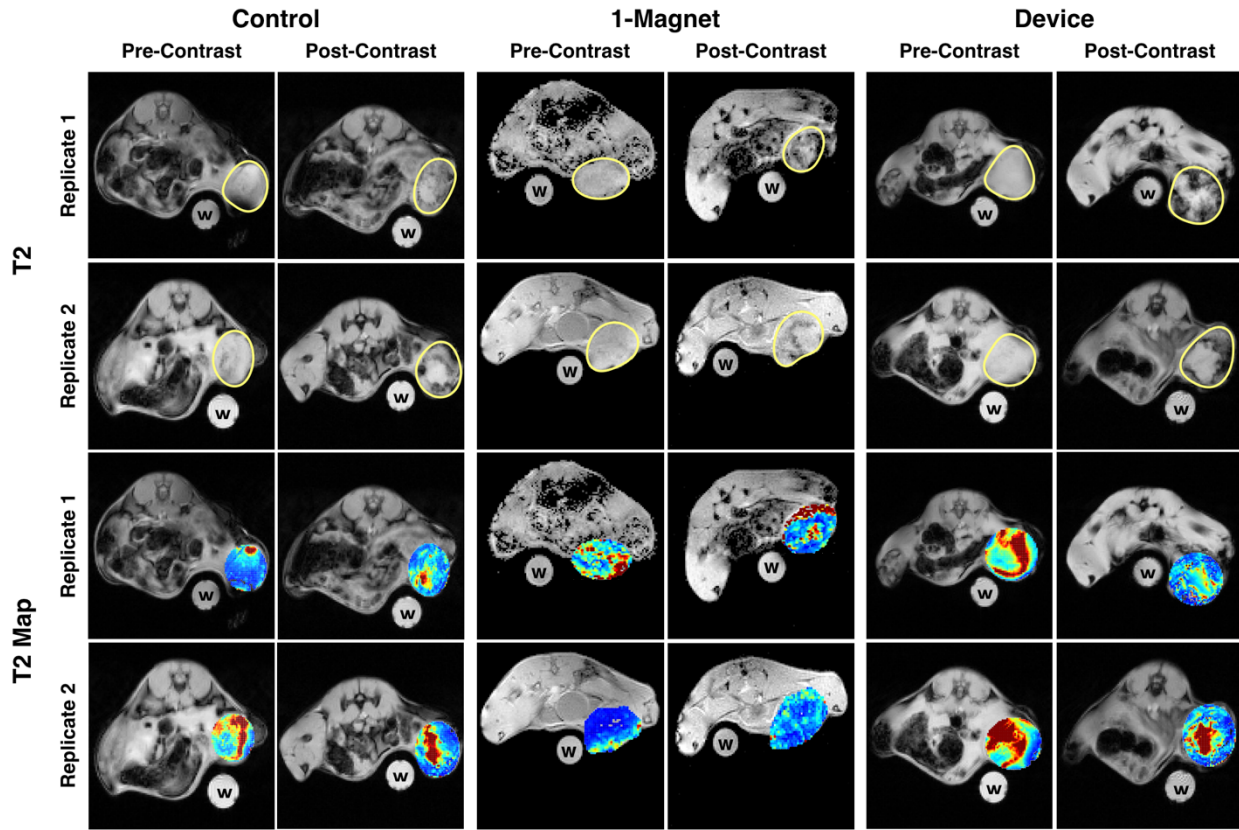


Figure S7. Additional MRI images showing T2 contrast and T2 maps pre- and post-injection in the device-exposed and control animals. There is some reduction in T2 signal and T2 time in tumors in control and 1-magnet-exposed animals. However, there is a greater reduction in T2 signal and T2 time in tumors in device-exposed animals. Water control labeled ‘w’. Scale bar = 5 mm. Images for replicate 3 shown in Fig. 7 of main text.

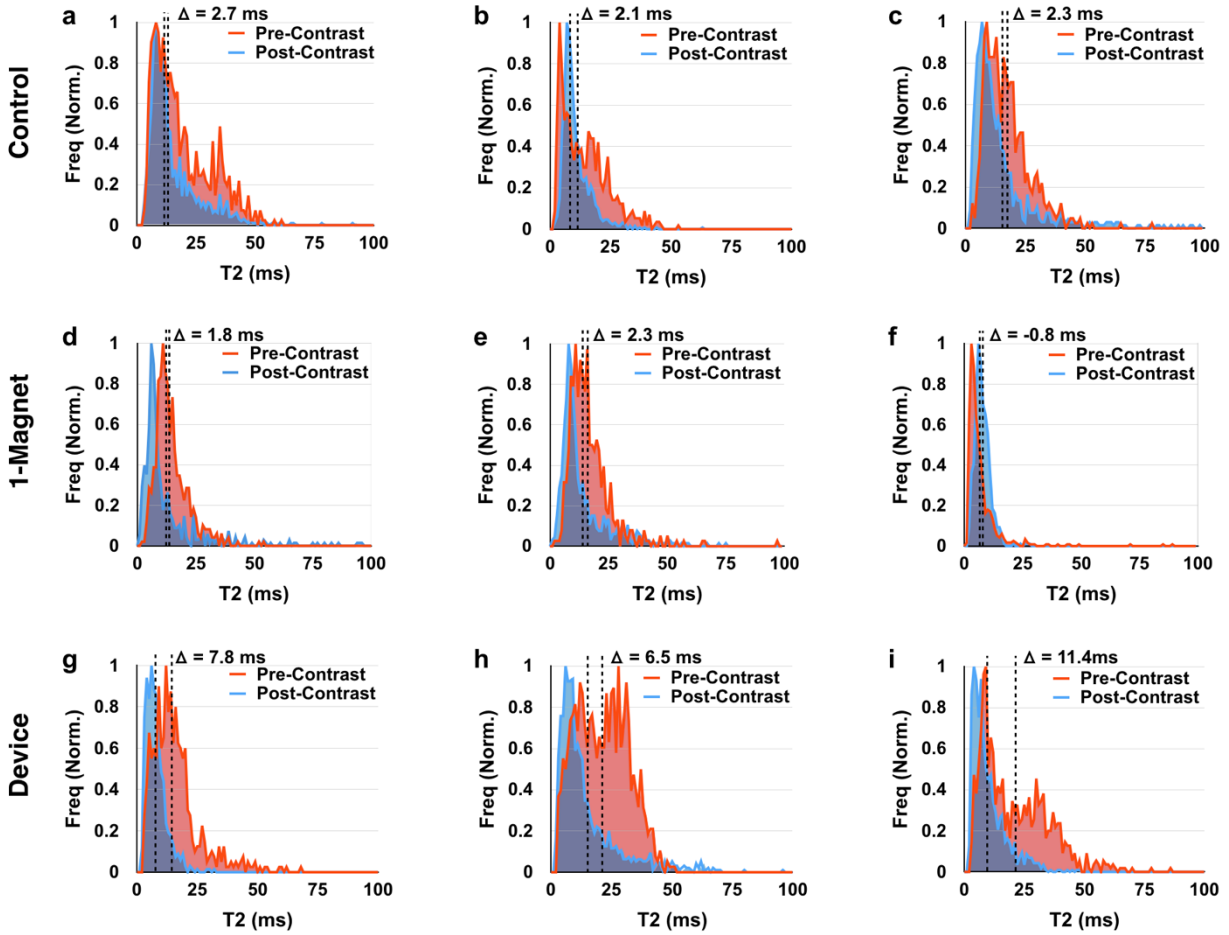


Figure S8. Histograms showing T2 time distributions in tumors pre- and post contrast in three individual control (a-c), three 1-magnet-exposed (d-f) and three device-exposed (g-i) animals (one histogram shown for each animal). The average T2 time reduction is 3.2 ms in control animals and 2.1 ms in 1-magnet-exposed animals, but > 7.5 ms in device animals.